PERK-mediated induction of miR-5p and miR-3p arms of miR-616 regulates cell growth by targeting c-MYC

Afrin Sultana[1†], Ananya Gupta[2] and Sanjeev Gupta[1*]

[1] Discipline of Pathology, School of Medicine, Clinical Science Institute, Lambe Institute for Translational Research, University of Galway, Galway, Ireland

[2] Discipline of Physiology, School of Medicine, University of Galway, Galway, Ireland

*Corresponding author
Email: sanjeev.gupta@universityofgalway.ie

Keywords: unfolded protein response, ER stress, miR-616, c-MYC, breast cancer

ABSTRACT

C/EBP homologous protein (CHOP), also known as DNA damage-inducible transcript 3 (DDIT3), is a member of CCAAT/enhancer-binding protein (C/EBP) family. The expression of CHOP is upregulated during unfolded protein response (UPR), and sustained CHOP activity plays an important role in UPR-induced apoptosis. MicroRNA-616 is localized in an intron of the CHOP gene. However, regulation of miR-616 expression during UPR and its function in breast cancer is not clearly understood. We show that miR-5p/-3p arms of miR-616 are expressed with levels of 5p arm higher than 3p arm. During conditions of UPR, the expression of miR-5p and miR-3p arms of miR-616 and its host gene (CHOP) was concordantly increased primarily in a PERK-dependent manner. We show that ectopic expression of miR-616 significantly suppressed cell growth and colony formation, whereas knockout of miR-616 increased it. We identified that MYC proto-oncogene (c-MYC) gene is repressed during the UPR and targeted by miR-616. Further, we show that expression of miR-616 and CHOP is downregulated in human breast cancer, where expression of miR-616 was associated with poor overall survival (OS) in luminal A subtype and better OS HER2 subtype of breast cancer. In summary, our results suggest a dual function for the DDIT3 locus, where CHOP protein and miR-616 can co-operate to regulate cancer progression.

56 # INTRODUCTION

57 The endoplasmic reticulum (ER) is a crucial cellular organelle that plays important role in
58 folding and maturation of proteins that transit through the secretory pathway. Stimuli that
59 compromise the protein handling capacity of the ER activate an evolutionarily conserved
60 pathway known as unfolded protein response (UPR). Three major sensor molecules that
61 initiate the UPR are activating transcription factor 6 (ATF6), inositol-requiring enzyme 1α
62 (IRE1) and protein kinase RNA-like endoplasmic reticulum kinase (PERK) (1). During resting
63 state the activity of PERK, IRE1 and ATF6 is kept under control by interaction with ER
64 chaperone glucose-regulated protein 78 (GRP78); however, upon accumulation of misfolded
65 proteins in ER, GRP78 dissociates from these molecules, leading to their activation (2). Upon
66 dissociation with GRP78, IRE1 auto-phosphorylates and oligomerizes leading to the
67 activation of its endoribonuclease domain present in the cytosolic domain. Active IRE1
68 catalyses the unconventional splicing of XBP1 mRNA and regulated IRE1-dependent decay of
69 transcripts (RIDD) (3). While splicing of XBP1 mRNA is an adaptive response to UPR, RIDD
70 has many context dependent outcomes (3). ATF6 is a transmembrane protein located in the
71 ER membrane with an N-terminus cytoplasmic domain containing a DNA-binding motif and
72 a C-terminus ER-luminal domain that interacts with GRP78 (4). During UPR, ATF6 is relocates
73 from the ER to the Golgi compartment. In the Golgi, ATF6 is processed by intramembranous
74 proteolysis causing the release of the transcriptionally active N-terminal cytosolic domain,
75 p50ATF6 (5). During UPR, active PERK phosphorylates eukaryotic initiation factor 2α (eIF2α),
76 causing reduced translation initiation for a majority of cellular proteins and preferential
77 translation of a subset of mRNAs including activating transcription factor 4 (ATF4) (6, 7).
78 Phosphorylation of eIF2α leads to general translational block and preferential translation of

79 a subset of mRNAs including activating transcription factor 4 (ATF4) (7). Phosphorylation of
80 NRF2 by PERK attenuates Keap1-mediated degradation of NRF2 and promotes expression of
81 NRF2-target genes through the antioxidant response elements (ARE) (6). The increased
82 protein handling capacity of the ER and degradation of unfolded proteins induced by UPR
83 attempts to restore the protein homeostasis and increase cell survival. However, if UPR-
84 induced mechanisms fail to alleviate ER stress, UPR activates apoptosis.
85
86 MicroRNAs (miRNAs) are small (~20–23 nucleotide) single-stranded RNA molecules that
87 regulate gene expression in a sequence-specific manner (8). The increased expression of
88 miR-616 has been reported in androgen-independent prostate cancer (9, 10), gastric cancer
89 (11), non-small cell lung cancer (NSCLC) (12), hepatocellular carcinoma (HCC) (13) and
90 gliomas (14). MiR-616 targets tissue factor pathway inhibitor (TFPI-2) in prostate cancer (9);
91 PTEN in HCC and gastric cancer (15); SOX7 in glioma and NSCLC (14). However, miR-616-3p
92 has been reported to reduce XIAP expression and potentiate apoptosis in HUVECs (16).
93 LINC01614 promotes head and neck squamous cell carcinoma progression via PI3K/AKT
94 signalling pathway and miR-616-3p can inhibit cancer progression by downregulating
95 LINC01614 expression (17). Ye et al. reported that miR-616-3p inhibited cell growth and
96 mammosphere formation of breast cancer cells by suppressing GLI1 (18), while Yuan
97 reported that miR-616-3p promoted breast cancer cell migration and invasion by targeting
98 TIMP2 and regulating MMP signalling (19). Overall, these observations suggest that miR-616
99 exhibits both oncogenic and tumour suppressor functions in context- and/or tissue-
100 dependent manner. Additional studies are warranted to further investigate the role of miR-
101 616 in human cancers.
102

103 During the past few years, work from several groups has revealed that all three branches of
104 the UPR regulate specific subsets of miRNAs (20, 21, 22, 23). The modes of regulation
105 include both increase and decrease in expression by UPR-regulated transcription factors
106 such as ATF6, XBP1, ATF4 and NRF2 as well as degradation by RIDD activity. The key feature
107 of UPR-dependent miRNA expression is fine tuning of the ER homeostasis to modulate
108 cellular adaptation to stress and regulation of cell fate. The gene encoding miRNA-616 is
109 located in the second intron of CHOP/DDIT3. This genomic co-location of miR-616 with
110 CHOP/DDIT3 suggests a role for miR-616 in UPR. Indeed, increased expression of miR-616
111 has been reported during conditions of UPR (24, 25). Hiramatsu et al., focused on the
112 expression of miR-616-5p (24) while Arabkari focused on the expression of miR-616-3p (25).
113 Here we have evaluated the expression of both miR-5p/-3p arms of miR-616 as well its host
114 gene (CHOP) during conditions of UPR.
115
116 We show that expression level of miR-616-5p was higher than miR-616-3p in human cancer
117 cells and tissues. During conditions of UPR, the expression of both miR-5p/-3p arms of miR-
118 616 and CHOP was increased in a PERK-dependent manner. Our results show that miR-616
119 regulates cell growth and proliferation along with regulation of c-MYC expression. We
120 identified that MYC proto-oncogene (MYC) gene is repressed during the UPR and targeted
121 by miR-616. Finally, we show that expression of miR-616 and CHOP (host gene of miR-616)
122 is reduced in human breast cancer. In summary, our results suggest that CHOP locus
123 generates two gene products, where CHOP protein and miR-616 can act together to
124 regulate cancer progression.
125

126 # METHODS

127 **Cell culture and treatments** - Human breast cancer cells (MCF7 and BT474) were purchased
128 from ECACC. HCT116 cells were kind gift from Dr. Victor E. Velculescu, Johns Hopkins
129 University, USA. HEK 293T cells were gift from Indiana University National Gene Vector
130 Biorepository. The MCF7, BT474 and HEK 293T cells were maintained in Dulbecco's modified
131 eagle's medium. HCT116 cells were maintained in McCoy's 5A modified. The medium was
132 supplemented with 10% heat inactivated foetal bovine serum (FBS) and 100 U/ml penicillin
133 and 100 µg/ml streptomycin with 5% CO2 at 37°C. Thapsigargin (Cat # 1138) and BFA (Cat #
134 1231) were purchased from Tocris Bioscience. All reagents were purchased from Sigma-
135 Aldrich unless otherwise stated.
136
137 **Plasmid constructs** - miExpressTM precursor miRNA expression clones, miR-CTRL and miR-
138 616 (pEZX-MR03 vector) were sourced from GeneCopoeia, Rockville, MD, USA. The lentiviral
139 plasmids pLV [CRISPR]-hCas9:T2A: Puro-U6>mir-616 expressing hCas9 protein and miR-616
140 targeting gRNA were obtained from VectorBuilder Inc, Chicago, IL, USA. The sequences of
141 two miR-616 targeting gRNAs are 5'-GGAAATAGGAAGTCATTGGA-3' and 5'-
142 GTGTCATGGAAGTCACTGAA-3'. PCDH-Flag-c-MYC was a gift from Hening Lin (Addgene
143 plasmid # 102626; http://n2t.net/addgene:102626; RRID: Addgene_102626).
144
145 **Generation of stable cell lines –** MCF7 cells were transduced with lentiviruses to generate
146 stable miR-616 overexpressing and miR-616 knockout sub-clones. Lentivirus was generated
147 by transfecting lentiviral plasmids along with packaging plasmids in 293T cells using jetPEI
148 transfection reagent as described previously (26).
149

150 **RNA extraction, Reverse transcription reaction and real time quantitative PCR** - Total RNA
151 was isolated using Trizol (Life Technologies) according to the manufacturer's instructions.
152 RPLP0 and GAPDH (for mRNAs) and U6 SnRNA (for miRNAs) were used as a reference genes
153 to determine the relative expression level of target genes between treated and control
154 samples using △△Ct method.
155
156 **Colony formation assay** - The cells were plated in 6 well plates and were grown for 14 days.
157 After 14 days, cells were washed twice with PBS and fixed with 10% formaldehyde for 5
158 minutes and stained with 0.5 % crystal violet for 10 minutes. The number of colonies were
159 counted in five random view fields under a microscope and average number of colonies was
160 determined. Colony size was determined using Image J software.
161
162 **X-CELLigence cell proliferation assay** - xCELLigence experiments were performed using the
163 Real-Time Cell Analyzer (RTCA) Dual Plate (DP) instrument according to the manufacturer's
164 instructions (Agilent.com). Briefly, instrument-specific specially designed gold
165 microelectrodes fused microtiter 16-well cell culture plate (0.2 cm2 well surface area; 250 µl
166 volume per well) was used to monitor the real-time changes expressed as Cell index (CI).
167 Cell Index is defined as (Rn−Rb)/15 where Rn is the cell–electrode impedance of the well
168 with the cells and Rb is the background impedance of the well with the medium alone. The
169 background impedance was measured by adding 50 µl of medium to each well of the E-Plate
170 before seeding the cells. After seeding (2500 cells/well), the E-plate was incubated at room
171 temperature for 30 min and then transferred to the instrument. Cell proliferation was
172 monitored every 15 min for 50 h.
173

174 **Western blot analysis** - Western blotting procedure has been described previously. After
175 blocking with specific solution nitrocellulose membranes were treated with specific primary
176 antibodies including c-MYC (Santa Cruz Biotechnology Cat# sc-40), ERα (Merck Millipore
177 Cat# 2828587) and β-Actin (Sigma, Cat# A-5060) at 4°C for overnight. After washing three
178 times with PBS/0.05%Tween solution, the membranes were incubated with appropriate
179 secondary antibody at room temperature for 2 hours. The membranes were then washed
180 twice with PBS/0.05%Tween and once with PBS and finally the signals were detected using
181 Western Lightening chemiluminescent substrate (Perkin Elmer, Netherlands, Cat
182 #NEL104001EA).
183
184 **Statistical Analysis** - The GraphPad was used for statistical analysis and generating graphs.
185 Two-tailed unpaired t-test was performed to determine statistically significant differences
186 between independent groups. Results with a $p<0.05$ were considered statistically significant.
187

188 # Results

189 ## Expression of miR-616-5p is higher than miR-616-3p

190 Several miRNAs are located within the introns of either protein coding or non-coding genes,
191 and are referred to as intronic miRNAs (27). The genes which harbour these miRNAs are
192 embedded are called host genes. MiR-616 is an intronic miRNA localized in the first intron of
193 DDIT3 gene (**Fig 1A**). Both the 5' and 3' arms of the precursor duplex can generate mature
194 miRNAs, and are referred to as miRNA-5p and -3p (27, 28). The miRBase
195 (http://www.mirbase.org) (29) has discontinued the use of miRNA/miRNA* nomenclature
196 and use of miR-5p and miR-3p nomenclature (30), based solely on 5'- or 3'-arm derivation of

197 the mature miRNA is now recommended. The sequences of mature miR-616, accession
198 numbers and the previous names of miR-616-5p and -3p as per miRNA/miRNA*
199 nomenclature are shown in Fig 1B. Indeed, both 5p and 3p arms of miR-616 have been
200 shown to be expressed in human cancers (11, 31). Next we evaluated the expression of miR-
201 616-5p and miR-616-3p in human cancers. Initially expression of miR-616-5p and miR-616-
202 3p was determined in various human cancer cell lines by qRT-PCR. We observed that
203 endogenous expression of miR-616-5p was higher than miR-616-3p in all the cell lines tested
204 (**Fig 1C**). Next we analysed the expression of miR-616-5p and miR-616-3p in the TCGA
205 dataset from different human cancers using OncomiR (http://www.oncomir.org), a web-
206 based tool for miRNA expression analysis. We observed a higher expression of miR-616-5p
207 as compared to miR-616-3p in all the cancer types evaluated (**Fig 2**). Of note the ratio of
208 miR-616-5p and miR-616-3p expression varied considerably across the different tissue
209 types. These results suggest that both 5p and 3p arms of miR-616 are expressed where miR-
210 616-5p accumulates at higher levels than miR-616-3p but their ratio is controlled in tissue-
211 specific manner.
212

213 **Fig 1. Basal expression of miR-616-5p and miR-616-3p in human cancer cell lines**. (A)
214 Schematic representation of the CHOP locus is shown. The exons are shown in blue and gray
215 line between them represents intron. The miR-616 is located in the first intron. The arrows
216 show the direction of transcription of the gene. The protein coding regions are shown in
217 dark blue and untranslated regions are shown in light blue. (B) The name, accession number
218 and sequence of miR-616-5p and 3p are shown. (C) Total RNA from indicated cells was used
219 to determine the expression of miR-616-5p and miR-616-3p by qRT-PCR and normalised
220 against RNU6. Expression of miR-616-3p in MCF7 cells was arbitrarily set at 1. Error bars
221 represent mean ±S.D. from three independent experiments performed in triplicate. *P <
222 0.05, two-tailed unpaired t-test compared to miR-616-3p in MCF7 cells.
223
224 **Fig 2. Expression of miR-616-5p and miR-616-3p in human cancers**. Web-based algorithm
225 at (http://www.oncomir.org/) was used to assess the expression of miR-616-5p and miR-
226 616-3p. Log2 mean expression of miR-616-5p and 3p in indicated cancer types is shown. (N
227 = number samples in each cancer type). ACC: adrenocortical carcinoma; BLCA: bladder

228 urothelial carcinoma; BRCA: breast invasive carcinoma; CESC: cervical squamous cell
229 carcinoma and endocervical adenocarcinoma; CHOL: cholangiocarcinoma; COAD: colon
230 adenocarcinoma; ESCA: esophageal carcinoma; HNSC: head and neck squamous cell
231 carcinoma; KICH: kidney chromophobe; KIRC: kidney renal clear cell carcinoma; KIRP: kidney
232 renal papillary cell carcinoma; LGG: brain lower grade glioma; LIHC: liver hepatocellular
233 carcinoma; LUAD: lung adenocarcinoma; LUSC: lung squamous cell carcinoma; MESO:
234 mesothelioma; OV: ovarian serous cystadenocarcinoma; PAAD: pancreatic
235 adenocarcinoma; PCPG: pheochromocytoma and paraganglioma; PRAD: prostate
236 adenocarcinoma; READ: rectal adenocarcinoma; SARC: sarcoma; SKCM: skin cutaneous
237 melanoma; STAD: stomach adenocarcinoma; TGCT: testicular germ cell tumours; THCA:
238 thyroid carcinoma; THYM: thymoma; UCEC: uterine corpus endometrial carcinoma; UCS:
239 uterine carcinosarcoma; UVM: uveal melanoma
240
241
242 **Increased expression of miR-616-5p and miR-616-3p during UPR**

243 It was initially proposed that intronic miRNAs are derived from the same primary transcript
244 as their host genes thereby leading to co-expression and co-regulation of miRNA and
245 cognate host gene (27). Analysis of expression of 175 miRNAs and their host genes across
246 twenty four different human organs reported a significantly correlated expression profile
247 (32). Recent evidence however, shows significant discordant expression between intronic
248 miRNAs and host genes. Two likely explanations for this discordant expression are: (i)
249 miRNAs have their own independent promoters and (ii) crosstalk between microprocessor
250 cleavage and mRNA splicing (33, 34)**.** Next, we evaluated the co-regulation of miR-616 and
251 its host gene (CHOP) during conditions of UPR. MCF7, BT474 and HCT116 cells were either
252 treated or untreated with thapsigargin (TG) or Brefeldin A (BFA) for 24 hours and expression
253 of CHOP, miR-616-5p and miR-616-3p was determined. The expression level of CHOP, miR-
254 616-5p and miR-616-3p was upregulated in all three cell lines tested, during ER stress (**Fig.**
255 **3A-C**). Next we investigated the role of ATF6, PERK and IRE1, three key mediators of the UPR
256 in upregulation of miR-616 expression. For this purpose, we used MCF7 control (MCF7
257 PLKO) and knockdown of UPR sensors (MCF7 XBP1-KD, MCF7 PERK-KD and MCF7 ATF6-KD)
258 sub-clones of MCF7 (35). We found that BFA-induced increase in the expression of CHOP,

259 pri-miR-616, miR-616-5p and miR-616-3p was attenuated in PERK-knockdown sub-clones of
260 MCF7 (**Fig 4A**), whereas knockdown of ATF6 or XBP1 had no significant effect (**Fig 4B-C**).
261 These results suggest that miR-616 is co-transcribed along with the CHOP transcript and
262 attenuated PERK signalling compromised the induction of CHOP mRNA, pri-miR-616, miR-
263 616-5p and miR-616-3p during UPR.
264

265 **Fig 3. Upregulation of miR-616 (5p and 3p) and its host gene CHOP during UPR.** (A) MCF7
266 cells, (B) BT474 cells and (C) HCT116 cells were treated with (1 µM) TG or (0.5 µg/ml) BFA
267 for 24 hours. Expression of CHOP was quantified by RT-qPCR, normalized using RPLP0. The
268 expression level of miR-616 -5p and -3p was quantified by RT-qPCR, normalized using U6
269 snRNA. Error bars represent mean ±S.D. from three independent experiments performed in
270 triplicate. *P < 0.05, two-tailed unpaired t-test as compared to untreated control.
271

272 **Fig 4. Upregulation of miR-616 during ER stress is dependent on PERK pathway.** (A-C)
273 MCF7 PLKO, MCF7 XBP1-KD, MCF7 PERK-KD and MCF7 ATF6-KD sub-clones were treated
274 with (0.5 µg/ml) BFA for 24 hours. Expression level of CHOP and pri-miR-616 was quantified
275 by RT-qPCR, normalizing against RPLP0. The expression level of miR-616 -5p and -3p was
276 quantified by RT-qPCR, normalized using U6 snRNA. *P<0.05, **P < 0.001, two-tailed
277 unpaired t-test. N.S not significant.
278

279 MiR-616 targets c-MYC and reduces cell proliferation of breast cancer cells

280 Ye et al. reported that ectopic expression of miR-616-3p inhibited growth of MDA-MB231
281 cells while Arabkari did not find any effect of miR-616 overexpression in MDA-MB231 cells
282 (18) (25). Further, Yuan reported that miR-616-3p promoted growth and migration of MCF7
283 cells in contrast to Arabkari, who reported a decrease in growth and migration of miR-616
284 expressing MCF7 cells (19) (25). This could be due to different approaches used for
285 overexpression of miRNAs. Next, we used gain-of-function (overexpression) and loss-of-
286 function (CRISPR-Cas9 KO) approaches in MCF7 cells to study the role of miR-616 in breast
287 cancer. To better mimic the *in vivo* scenario we decided to use a lentiviral system for
288 modulating the expression of both miR-616-5p and -3p concurrently. For this purpose,

289 MCF7 cells were transduced with lentivirus expressing GFP along with miR-616 or Cas-9
290 along with gRNAs targeting miR-616. The expression of pri-miR-616, miR-616-5p and miR-
291 616-3p was determined in miR-616-overexpressing (MCF7-miR-616-OE) and miR-616-
292 knockout (MCF7-miR-616-KO) sub-clones of MCF7. As expected, the levels of pri-miR-616,
293 miR-616-5p and miR-616-3p were increased in MCF7-miR-616-OE sub-clone (**Fig. 5A**) and
294 decreased in MCF7-miR-616-KO sub-clone (**Fig. 5E**). The MCF7-miR-616-KO sub-clone
295 displayed hypomorphic phenotype with partial reduction in expression of pri-miR-616, miR-
296 616-5p and miR-616-3p. The miR-616 overexpressing (MCF7-miR-616-OE) sub-clone showed
297 significantly decreased cell growth (**Fig. 5B**), while the miR-616 knockout (MCF7-miR-616-
298 KO) sub-clone showed increased cell growth (**Fig. 5F**). This observation was further validated
299 by colony formation assay. The miR-616 overexpressing (MCF7-miR-616-OE) sub-clone of
300 MCF7 cells showed decrease in the number and size of the colonies (**Fig. 5C-D**) but miR-616
301 knockout (MCF7-miR-616-KO) sub-clone showed an increase in the number and size of the
302 colonies (**Fig. 5G-H**). We found that expression of c-MYC mRNA and protein was reduced
303 miR-616 overexpressing (MCF7-miR-616-OE) sub-clone of MCF7 cells (**Fig. 6 A and C**) and
304 increased in miR-616 knockout (MCF7-miR-616-KO) sub-clone (**Fig. 6 B and C**). Our results
305 are in agreement with an earlier report where ectopic expression of miR-616 was shown to
306 inhibit growth of MCF7 cells accompanied by reduced expression of c-MYC (25). Since an
307 inverse relationship between the levels of expression of a miRNA and its target is
308 anticipated, we evaluated expression of c-MYC during conditions of UPR. We found the
309 expression of c-MYC mRNA was decreased in MCF7 (**Fig. 7A)** and BT474 (**Fig. 7B**) cells
310 treated either with TG or BFA. Furthermore, expression of c-MYC protein was decreased in
311 MCF7 and BT474 cells upon treatment with BFA (**Fig. 7C**). These results suggest a role for
312 miR-616 in regulation of c-MYC expression during conditions of UPR.

313 **Fig 5. MiR-616 reduces the proliferation of MCF7 cells.** (A) The expression of miR-616-3p,
314 miR-616-5p and pri-miR-616 is shown in MCF7-miR-CTRL and MCF7-miR-616-OE sub-clones
315 of MCF7. (B) MCF7-miR-CTRL and MCF7-miR-616-OE cells were plated and cell growth was
316 determined by x-CELLigence. (C-D) MCF7-miR-CTRL and MCF7-miR-616-OE cells were plated
317 in 6- well plate (1000 cells/well) and grown for 14 days. (C) Colonies stained with crystal
318 violet are shown. (D) Quantification of number of colonies for MCF7-miR-CTRL and MCF7-
319 miR-616-OE cells is shown. (E) The expression of miR-616-3p, miR-616-5p and pri-miR-616 is
320 shown in MCF7-Cas9-CTRL and MCF7-miR-616-KO sub-clones of MCF7. (F) MCF7-Cas9-CTRL
321 and MCF7-miR-616-KO cells were plated and cell growth was determined by x-CELLigence.
322 (G-H) MCF7-Cas9-CTRL and MCF7-miR-616-KO cells were plated in 6-well plate (1000
323 cells/well) and grown for 14 days. (G) Colonies stained with crystal violet are shown. (H)
324 Quantification of number of colonies for MCF7-Cas9-CTRL and MCF7-miR-616-KO cells is
325 shown.
326
327
328 **Fig 6. MiR-616 regulates the expression of c-MYC.** (A-B) Expression level of c-MYC mRNA is
329 shown in miR-616 knockout and miR-616 overexpressing sub-clones of MCF7 cells as
330 determined by qRT-PCR. Error bars represent mean ± S.D. from two independent
331 experiments performed in triplicate. *P < 0.05, two-tailed unpaired t-test as compared to
332 control. (C) The expression level of c-MYC protein is shown in miR-616 knockout and miR-
333 616 overexpressing sub-clones of MCF7 cells.
334
335 **Fig 7. Downregulation of c-MYC during UPR in breast cancer cells.** (A) MCF7 cells and (B)
336 BT474 cells were treated with (1 µM) TG or (0.5 µg/ml) BFA for 24 hours. Expression of c-
337 MYC was quantified by RT-qPCR, and normalized using RPLP0. Error bars represent mean
338 ±S.D. from three independent experiments performed in triplicate. (C) MCF7 BT474 cells
339 were treated with (0.5 µg/ml) BFA for indicated time points. Western blotting of total
340 protein was performed using antibodies for c-MYC and actin. Representative Immunoblot
341 and quantification of c-MYC expression normalised to actin are shown (n=3). *P < 0.05, two-
342 tailed unpaired t-test as compared to the untreated control.
343

344 MiR-616 modulates the expression of c-MYC via site in the ORF

345 To determine the mechanism of c-MYC regulation by miR-616, we used several
346 bioinformatics tools to search for the potential miR-616 binding sites in the reference
347 sequence of c-MYC. TargetScan (36) did not identify miR-616 binding sites in c-MYC.
348 Interestingly, RNAhybrid identified non-canonical miR-616-5p binding sites (at position 77,
349 2501 and 3076 bp) and miR-616-3p binding sites (at position 614, 917 and 1525 bp) of c-
350 MYC reference Sequence (NM_002467.6) (**S1 Fig**). Furthermore, (miRWALK and RNAhybrid)

351 picked an identical, non-canonical miR-616-3p binding site in the protein-coding region
352 (364-1728 bp) of c-MYC at position 1525 bp (**Fig. 8A-B**). To test whether miR-616 down-
353 regulates c-MYC via this site in coding region, we co-transfected 293T cells with an
354 expression vector containing the ORF of c-MYC and miR-616 plasmid. Cell lysates were
355 collected after 24 h and analysed by immunoblotting. Our results showed that c-MYC
356 protein level was strongly down-regulated by co-expression of miR-616 (**Fig. 8C**). Under
357 similar conditions, co-expression of miR-616 had no effect on protein level of ERα (protein
358 coding region of ERα has no predicted binding sites for miR-616) (**Fig. 8D**). Further, co-
359 expression of miR-4726 (miRNA that lacks binding sites in the protein coding region of c-
360 MYC) and c-MYC had no effect on c-MYC protein level (**Fig. 8E**). Taken together these results
361 suggest that miR-616 regulates the expression of c-MYC most likely via the miR-616
362 response elements present in its protein coding region.
363

364 Fig 8. **Identification of a miR-616-3p-binding sites in the ORF of c-MYC.** Binding site for
365 miR-616-3p identified by (A) miRWALK and (B) RNAhybrid in protein coding region of c-MYC
366 reference sequence is shown. The secondary structure of miRNA-mRNA duplex is shown
367 with miR-616-3p in green and c-MYC mRNA in red. mfe: minimum free energy. (C) 293T cells
368 were transfected with plasmid containing c-MYC ORF in absence and presence of miR-616
369 plasmid. (D) 293T cells were transfected with plasmid containing ERα ORF in absence and
370 presence of miR-616 plasmid. (E) 293T cells were transfected with plasmid containing c-MYC
371 ORF in absence and presence of miR-4726 plasmid. Western blotting of total protein was
372 performed using the indicated antibodies. 24 h post-transfection western blotting of total
373 protein was performed using the indicated antibodies.
374

375 Prognostic value of the miR-616 in human cancers

376 We assessed the prognostic value of miR-616 in different cancer types using KM plotter. We
377 found that expression of miR-616 was associated with longer overall survival (OS) in cervical
378 squamous cell carcinoma, Head-neck squamous cell carcinoma, uterine corpus endometrial
379 carcinoma and Thymoma (**S2 Fig**). Surprisingly, the increased expression of miR-616 was

380 associated with shorter OS in esophageal adenocarcinoma, sarcoma, renal clear cell
381 carcinoma, lung squamous cell carcinoma and hepatocellular carcinoma (**S2 Fig**). Next, we
382 used TNMplot to determine the expression of CHOP and miR-616 in normal and tumour
383 tissue samples of breast. We found that expression of CHOP and miR-616 was reduced in
384 tumour samples as compared to tumour adjacent normal tissue (**Fig 9A-B**). Further, the
385 expression of miR-616 was associated with poor OS in luminal A subtype and better OS
386 HER2 subtype of breast cancer (**Fig 9C**).

387 **Fig 9. Prognostic value of miR-616 in subtypes of breast cancer.** TNMplot
388 (https://tnmplot.com/analysis/) was used to determine the expression of CHOP and miR-
389 616 in human breast cancer. (A) Box plot for expression of CHOP in tumour (n=1097) and
390 normal (n=403) tissues for human breast cancers is shown. (B) Box plot for expression of
391 miR-616 in paired tumour (n=112) and tumour adjacent normal (n=112) for human breast
392 cancers is shown. (C) KM Plotter (https://kmplot.com/) was used to determine the
393 association of miR-616 with overall survival (OS) in subtypes of breast cancer.
394

395 # DISCUSSION

396 MiRNAs regulate the wide range of cellular processes because of their ability to alter post-
397 transcriptional gene expression (37). We have evaluated the role of UPR regulated miRNA-
398 616 in cell growth and proliferation. We have shown that expression of miR-616 and its host
399 gene (CHOP) is upregulated during ER stress in a PERK-dependent fashion (**Fig 4**). ER stress
400 and UPR activation contributes to the initiation and progression of human diseases, such as
401 cancer, neurodegenerative and cardiovascular disease (2, 38). We observed concordant
402 expression of the CHOP and the mature miR-616 which suggests their transcriptional co-
403 regulation (**Fig 3, 4**). Our results suggest a mechanism for increased expression of miR-616
404 in patho-physiological conditions where role of UPR is implicated.
405

406 Several studies have reported that miR-616 acts as a tumour promoting miRNA in human
407 cancers (11, 31, 39). However, our results show that miR-616 expression attenuates the
408 proliferation of MCF7 cells while reduced expression of miR-616 increases it (**Fig 5**).
409 Furthermore, we observed that expression of miR-616 was reduced in human breast
410 cancers as compared to tumour adjacent normal tissue (**Fig 9**). In agreement with our
411 results miR-616-3p has been shown to potentiate apoptosis in HUVECs (16), inhibit head
412 and neck squamous cell carcinoma progression (17) and inhibit cell growth and
413 mammosphere formation of breast cancer cells (18, 25). Any small RNA having G-rich 6mer
414 seed sequence (nt 2-7 of the guide strand) can reduce viability of cells when associated with
415 RNA-induced silencing complex. G-rich seed sequence mediates toxicity by targeting C-rich
416 seed matches in the 3′ UTR of genes critical for cell survival referred to as Death Induced by
417 Survival gene Elimination (DISE) (30). A systematic study to evaluate DISE activity of all 4096
418 possible 6mer seed sequences in six cell lines (three human and three mouse) revealed the
419 mechanism underlying this toxicity and a web-based algorithm (https://6merdb.org) can
420 predict the activity of an RNA with a known 6mer seed (40). Analysis of seed sequences
421 from both 5p and 3p strands of miR-616 revealed that both strands can exhibit opposing
422 effects on viability in a cell-type dependent manner (**S3 Fig**). Interestingly, several miRNAs
423 belonging to miR-371-373 Cluster (hsa-miR-371a-5p, hsa-miR-371b-5p, hsa-miR-372-5p and
424 hsa-miR-373-5p) that share seed sequence with miR-616-5p, have been shown to reduce
425 the progression and metastasis of colon cancer (41) as well as induction of cell cycle arrest
426 (42). Taken together, these observations indicate the presence of context-dependent
427 oncogenic and tumour suppressive effects of miR-616 in human cancers. Indeed context-
428 dependent tumour-promoting and tumour-suppressive role has been documented for
429 several miRNAs such as miR-17-92 cluster (43, 44). This cluster maps to a region frequently

430 amplified in Burkitt's lymphoma, diffuse large B-cell lymphoma, follicular lymphoma and
431 lung cancer (26, 43). The expression of miR-17-92 is reduced in prostate cancer (17) and
432 miR-17-92 expression in intestinal epithelial cells inhibited colon cancer progression by
433 suppressing tumour angiogenesis (17).
434
435 Studies on target recognition by miRNAs have shown that sequence complementarity at the
436 5' end of the miRNA, the so-called "seed region" at positions 2 to 7, is a main determinant
437 for target recognition (36). However, a perfect seed match of its own is not a good predictor
438 for miRNA regulation and a number of studies have shown that miRNA can regulate the
439 expression of target genes via the sites with a G: U wobble and/or mismatch in the seed
440 region (36). Further, a study using a cross-linking and immunoprecipitation method to
441 experimentally identify microRNA target sites in an unbiased manner has reported a
442 significant number of non-canonical sites (45, 46). Hence, presence of perfect seed
443 complementarity is not essential for regulation of target genes by miRNA. In addition, target
444 sites for endogenous miRNAs have been reported in ORFs and 5 UTRs, but they are less
445 frequent than those in the 3' UTR (47, 48). We found a non-canonical miR-616-3p binding
446 site in the protein coding region of c-MYC transcript (**Fig 8**). Several studies have reported
447 the presence of miRNA-binding sites in the protein coding sequence of the genes. Indeed
448 miRNAs have been shown to regulate embryonic stem cell differentiation, DNA methylation,
449 regulation of apoptosis, aortic development, and tumour suppression via the functional
450 miRNA-binding sites in the protein coding sequence of the target genes (47, 48, 49). Several
451 studies have reported the upregulation of c-MYC in different cancer cells and tumours such
452 as neuroblastomas, lung, and breast cancer (50). The expression of c-MYC was
453 downregulated in miR-616 expressing and upregulated in miR-616 knockout MCF7 cells (**Fig**

454 **6**). These observations suggest that effects of miR-616 on cell growth are primarily mediated
455 by downregulation of c-MYC.
456
457 PERK has been shown to act as a haploinsufficient tumour suppressor, where the nature of
458 its function is determined by gene dose (51, 52). Transient pause in protein synthesis due to
459 eIF2α phosphorylation by PERK is beneficial by reducing secretory load in the ER.
460 Phosphorylation of NRF2 by PERK attenuates Keap1-mediated degradation of NRF2 and
461 promotes expression of anti-oxidant enzymes through the antioxidant response elements
462 (53, 54). PERK signalling can upregulate the CHOP/DDIT3 transcription factor, which inhibits
463 expression of the gene encoding anti-apoptotic BCL-2 to hasten cell death, in addition to
464 enhancing the expression of pro-apoptotic BCL-2 members such as BIM (54). Studies in both
465 cellular and animal models with CHOP gene deficiency have shed light on the pro-apoptotic
466 role of CHOP during cellular stress (54). Further, ectopic expression of CHOP was reported to
467 induce a G1 cell cycle arrest (55). CHOP maintains the integrity of the human hematopoietic
468 stem cell (HSC) pool by eliminating HSCs harbouring oncogenic mutations, and decrease the
469 risk of leukaemia. CHOP induction triggers apoptosis of premalignant cells to prevent
470 malignant progression in a mouse lung cancer model. Hepatocyte-specific CHOP ablation
471 increased tumourigenesis in high fat diet-induced steatohepatitis and Hepatocellular
472 carcinoma (56, 57). CHOP has been shown to promote cancer progression, when fused with
473 FUS/TLS or EWS protein by genomic rearrangement (58, 59). The FUS-CHOP oncoprotein has
474 been shown to induce metastasis in in vivo model of sarcoma (58). Accumulating data
475 suggest that CHOP impinges upon several aspects of cancer including initiation as well as
476 progression of tumours (54). Our results show that miR-616 supressed cell growth of cancer
477 cells through suppressing c-MYC expression. Our results establish a new and unexpected

478 role for the CHOP locus by providing evidence that miR-616 can inhibit cell proliferation by
479 targeting c-MYC.
480

481 # ACKNOWLEDGEMENTS

482 We are grateful to the Technical Officers and administrative team in Pathology, School of
483 Medicine at University of Galway, Ireland.
484

485 # REFERENCES

486 1. Hetz C, Zhang K, Kaufman RJ. Mechanisms, regulation and functions of the unfolded protein
487 response. Nat Rev Mol Cell Biol. 2020;21(8):421-38.
488 2. Hetz C, Axten JM, Patterson JB. Pharmacological targeting of the unfolded protein response
489 for disease intervention. Nat Chem Biol. 2019;15(8):764-75.
490 3. Barua D, Gupta A, Gupta S. Targeting the IRE1-XBP1 axis to overcome endocrine resistance
491 in breast cancer: Opportunities and challenges. Cancer Lett. 2020;486:29-37.
492 4. Nadanaka S, Okada T, Yoshida H, Mori K. Role of disulfide bridges formed in the luminal
493 domain of ATF6 in sensing endoplasmic reticulum stress. Mol Cell Biol. 2007;27(3):1027-43.
494 5. Yoshida H, Okada T, Haze K, Yanagi H, Yura T, Negishi M, et al. ATF6 activated by proteolysis
495 binds in the presence of NF-Y (CBF) directly to the cis-acting element responsible for the mammalian
496 unfolded protein response. Mol Cell Biol. 2000;20(18):6755-67.
497 6. Cullinan SB, Zhang D, Hannink M, Arvisais E, Kaufman RJ, Diehl JA. Nrf2 is a direct PERK
498 substrate and effector of PERK-dependent cell survival. Mol Cell Biol. 2003;23(20):7198-209.
499 7. Harding HP, Zhang Y, Bertolotti A, Zeng H, Ron D. Perk is essential for translational regulation
500 and cell survival during the unfolded protein response. Mol Cell. 2000;5(5):897-904.
501 8. Ha M, Kim VN. Regulation of microRNA biogenesis. Nat Rev Mol Cell Biol. 2014;15(8):509-24.
502 9. Ma S, Chan YP, Kwan PS, Lee TK, Yan M, Tang KH, et al. MicroRNA-616 induces androgen-
503 independent growth of prostate cancer cells by suppressing expression of tissue factor pathway
504 inhibitor TFPI-2. Cancer Res. 2011;71(2):583-92.
505 10. Zhang S, Zhang X, Chen G, Zheng X, Zhu X, Shan L. Hsa_circ_0007494 suppresses prostate
506 cancer progression via miR-616/PTEN axis. Exp Cell Res. 2020;395(2):112233.
507 11. Wu ZH, Lin C, Liu CC, Jiang WW, Huang MZ, Liu X, et al. MiR-616-3p promotes angiogenesis
508 and EMT in gastric cancer via the PTEN/AKT/mTOR pathway. Biochem Biophys Res Commun.
509 2018;501(4):1068-73.
510 12. Wang DX, Zou YJ, Zhuang XB, Chen SX, Lin Y, Li WL, et al. Sulforaphane suppresses EMT and
511 metastasis in human lung cancer through miR-616-5p-mediated GSK3β/β-catenin signaling
512 pathways. Acta Pharmacol Sin. 2017;38(2):241-51.
513 13. Zhang D, Zhou P, Wang W, Wang X, Li J, Sun X, et al. MicroRNA-616 promotes the migration,
514 invasion and epithelial-mesenchymal transition of HCC by targeting PTEN. Oncol Rep.
515 2016;35(1):366-74.
516 14. Bai QL, Hu CW, Wang XR, Shang JX, Yin GF. MiR-616 promotes proliferation and inhibits
517 apoptosis in glioma cells by suppressing expression of SOX7 via the Wnt signaling pathway. Eur Rev
518 Med Pharmacol Sci. 2017;21(24):5630-7.

519 15. Fan MQ, Huang CB, Gu Y, Xiao Y, Sheng JX, Zhong L. Decrease expression of microRNA-20a
520 promotes cancer cell proliferation and predicts poor survival of hepatocellular carcinoma. J Exp Clin
521 Cancer Res. 2013;32(1):21.
522 16. Chen H, Liu X, Wu Y, Wu X, Wen X, Lu Y, et al. Apoptosis in HUVECs induced by microRNA-
523 616-3p via X-linked inhibitor of apoptosis protein targeting. Exp Ther Med. 2021;21(6):661.
524 17. Hou Y, Zhou M, Li Y, Tian T, Sun X, Chen M, et al. Risk SNP-mediated LINC01614 upregulation
525 drives head and neck squamous cell carcinoma progression via PI3K/AKT signaling pathway. Mol
526 Carcinog. 2022;61(8):797-811.
527 18. Ye G, Pan R, Zhu L, Zhou D. Circ_DCAF6 potentiates cell stemness and growth in breast
528 cancer through GLI1-Hedgehog pathway. Exp Mol Pathol. 2020;116:104492.
529 19. Yuan C. miR-616 promotes breast cancer migration and invasion by targeting TIMP2 and
530 regulating MMP signaling. Oncol Lett. 2019;18(3):2348-55.
531 20. Gupta A, Hossain MM, Read DE, Hetz C, Samali A, Gupta S. PERK regulated miR-424(322)-503
532 cluster fine-tunes activation of IRE1 and ATF6 during Unfolded Protein Response. Sci Rep.
533 2015;5:18304.
534 21. Gupta S, Read DE, Deepti A, Cawley K, Gupta A, Oommen D, et al. Perk-dependent
535 repression of miR-106b-25 cluster is required for ER stress-induced apoptosis. Cell Death Dis.
536 2012;3(6):e333.
537 22. Cawley K, Logue SE, Gorman AM, Zeng Q, Patterson J, Gupta S, et al. Disruption of microRNA
538 biogenesis confers resistance to ER stress-induced cell death upstream of the mitochondrion. PLoS
539 One. 2013;8(8):e73870.
540 23. Read DE, Gupta A, Ladilov Y, Samali A, Gupta S. miRNA signature of unfolded protein
541 response in H9c2 rat cardiomyoblasts. Cell Biosci. 2014;4(1):56.
542 24. Hiramatsu N, Chiang K, Aivati C, Rodvold JJ, Lee JM, Han J, et al. PERK-mediated induction of
543 microRNA-483 disrupts cellular ATP homeostasis during the unfolded protein response. J Biol Chem.
544 2020;295(1):237-49.
545 25. Arabkari V. *Regulation of cell fate by microRNAs during unfolded protein response*

546 *and its role in cancer* [Doctor of Philosophy]. Galway: National University of Ireland Galway, Ireland;
547 (2018) https://aran.library.nuigalway.ie/handle/10379/14750.
548 26. Hossain MM, Sultana A, Barua D, Islam MN, Gupta A, Gupta S. Differential expression,
549 function and prognostic value of miR-17-92 cluster in ER-positive and triple-negative breast cancer.
550 Cancer Treat Res Commun. 2020;25:100224.
551 27. Salim U, Kumar A, Kulshreshtha R, Vivekanandan P. Biogenesis, characterization, and
552 functions of mirtrons. Wiley Interdiscip Rev RNA. 2022;13(1):e1680.
553 28. Mitra R, Lin CC, Eischen CM, Bandyopadhyay S, Zhao Z. Concordant dysregulation of miR-5p
554 and miR-3p arms of the same precursor microRNA may be a mechanism in inducing cell proliferation
555 and tumorigenesis: a lung cancer study. RNA. 2015;21(6):1055-65.
556 29. Kozomara A, Griffiths-Jones S. miRBase: annotating high confidence microRNAs using deep
557 sequencing data. Nucleic Acids Res. 2014;42(Database issue):D68-73.
558 30. Putzbach W, Gao QQ, Patel M, Haluck-Kangas A, Murmann AE, Peter ME. DISE: A Seed-
559 Dependent RNAi Off-Target Effect That Kills Cancer Cells. Trends Cancer. 2018;4(1):10-9.
560 31. Ren W, Hu J, Li H, Chen J, Ding J, Zu X, et al. miR-616-5p Promotes Invasion and Migration of
561 Bladder Cancer. Front Oncol. 2021;11:762946.
562 32. Baskerville S, Bartel DP. Microarray profiling of microRNAs reveals frequent coexpression
563 with neighboring miRNAs and host genes. RNA. 2005;11(3):241-7.
564 33. Schanen BC, Li X. Transcriptional regulation of mammalian miRNA genes. Genomics.
565 2011;97(1):1-6.
566 34. Agranat-Tamir L, Shomron N, Sperling J, Sperling R. Interplay between pre-mRNA splicing
567 and microRNA biogenesis within the supraspliceosome. Nucleic Acids Res. 2014;42(7):4640-51.
568 35. Hossain MM, Barua D, Arabkari V, Islam N, Gupta A, Gupta S. Hyperactivation of nuclear
569 receptor coactivators induces PERK-dependent cell death. Oncotarget. 2018;9(14):11707-21.

570 36. Agarwal V, Bell GW, Nam JW, Bartel DP. Predicting effective microRNA target sites in
571 mammalian mRNAs. Elife. 2015;4.
572 37. Jin HY, Xiao C. MicroRNA Mechanisms of Action: What have We Learned from Mice? Front
573 Genet. 2015;6:328.
574 38. Doyle KM, Kennedy D, Gorman AM, Gupta S, Healy SJ, Samali A. Unfolded proteins and
575 endoplasmic reticulum stress in neurodegenerative disorders. J Cell Mol Med. 2011;15(10):2025-39.
576 39. Zhou Y, Meng P, Tang B, Ke Z, Liu L, Chen Y, et al. MiR-616 promotes the progression of
577 pancreatic carcinoma by targeting OXR1. Minerva Med. 2021;112(4):528-9.
578 40. Bartom ET, Kocherginsky M, Paudel B, Vaidyanathan A, Haluck-Kangas A, Patel M, et al.
579 SPOROS: A pipeline to analyze DISE/6mer seed toxicity. PLoS Comput Biol. 2022;18(3):e1010022.
580 41. Ullmann P, Rodriguez F, Schmitz M, Meurer SK, Qureshi-Baig K, Felten P, et al. The miR-
581 371~373 Cluster Represses Colon Cancer Initiation and Metastatic Colonization by Inhibiting the
582 TGFBR2/ID1 Signaling Axis. Cancer Res. 2018;78(14):3793-808.
583 42. Langroudi L, Jamshidi-Adegani F, Shafiee A, Rad SM, Keramati F, Azadmanesh K, et al. MiR-
584 371-373 cluster acts as a tumor-suppressor-miR and promotes cell cycle arrest in unrestricted
585 somatic stem cells. Tumour Biol. 2015;36(10):7765-74.
586 43. Zhao W, Gupta A, Krawczyk J, Gupta S. The miR-17-92 cluster: Yin and Yang in human
587 cancers. Cancer Treat Res Commun. 2022;33:100647.
588 44. Yu L, Ma W, Song B, Wang S, Li X, Wang Z. Hsa_circ_0030042 Ameliorates Oxidized Low-
589 Density Lipoprotein-Induced Endothelial Cell Injury via the MiR-616-3p/RFX7 Axis. Int Heart J.
590 2022;63(4):763-72.
591 45. Stavast CJ, Erkeland SJ. The Non-Canonical Aspects of MicroRNAs: Many Roads to Gene
592 Regulation. Cells. 2019;8(11).
593 46. Dai W, Su X, Zhang B, Wu K, Zhao P, Yan Z. An Alternative Class of Targets for microRNAs
594 Containing CG Dinucleotide. Biology (Basel). 2022;11(3).
595 47. Qin W, Shi Y, Zhao B, Yao C, Jin L, Ma J, et al. miR-24 regulates apoptosis by targeting the
596 open reading frame (ORF) region of FAF1 in cancer cells. PLoS One. 2010;5(2):e9429.
597 48. Duursma AM, Kedde M, Schrier M, le Sage C, Agami R. miR-148 targets human DNMT3b
598 protein coding region. RNA. 2008;14(5):872-7.
599 49. Tay Y, Zhang J, Thomson AM, Lim B, Rigoutsos I. MicroRNAs to Nanog, Oct4 and Sox2 coding
600 regions modulate embryonic stem cell differentiation. Nature. 2008;455(7216):1124-8.
601 50. Dang CV. MYC on the path to cancer. Cell. 2012;149(1):22-35.
602 51. Pytel D, Gao Y, Mackiewicz K, Katlinskaya YV, Staschke KA, Paredes MC, et al. PERK Is a
603 Haploinsufficient Tumor Suppressor: Gene Dose Determines Tumor-Suppressive Versus Tumor
604 Promoting Properties of PERK in Melanoma. PLoS Genet. 2016;12(12):e1006518.
605 52. Gupta S, Giricz Z, Natoni A, Donnelly N, Deegan S, Szegezdi E, et al. NOXA contributes to the
606 sensitivity of PERK-deficient cells to ER stress. FEBS Lett. 2012;586(22):4023-30.
607 53. Pytel D, Majsterek I, Diehl JA. Tumor progression and the different faces of the PERK kinase.
608 Oncogene. 2016;35(10):1207-15.
609 54. Oyadomari S, Mori M. Roles of CHOP/GADD153 in endoplasmic reticulum stress. Cell Death
610 Differ. 2004;11(4):381-9.
611 55. Jauhiainen A, Thomsen C, Strombom L, Grundevik P, Andersson C, Danielsson A, et al.
612 Distinct cytoplasmic and nuclear functions of the stress induced protein DDIT3/CHOP/GADD153.
613 PLoS One. 2012;7(4):e33208.
614 56. Toriguchi K, Hatano E, Tanabe K, Takemoto K, Nakamura K, Koyama Y, et al. Attenuation of
615 steatohepatitis, fibrosis, and carcinogenesis in mice fed a methionine-choline deficient diet by
616 CCAAT/enhancer-binding protein homologous protein deficiency. J Gastroenterol Hepatol.
617 2014;29(5):1109-18.
618 57. Rahman SM, Schroeder-Gloeckler JM, Janssen RC, Jiang H, Qadri I, Maclean KN, et al.
619 CCAAT/enhancing binding protein beta deletion in mice attenuates inflammation, endoplasmic

620 reticulum stress, and lipid accumulation in diet-induced nonalcoholic steatohepatitis. Hepatology.
621 2007;45(5):1108-17.
622 58. Pérez-Losada J, Pintado B, Gutiérrez-Adán A, Flores T, Bañares-González B, del Campo JC, et
623 al. The chimeric FUS/TLS-CHOP fusion protein specifically induces liposarcomas in transgenic mice.
624 Oncogene. 2000;19(20):2413-22.
625 59. Matsui Y, Ueda T, Kubo T, Hasegawa T, Tomita Y, Okamoto M, et al. A novel type of EWS-
626 CHOP fusion gene in myxoid liposarcoma. Biochem Biophys Res Commun. 2006;348(2):437-40.

627

628 Supporting information

629 S1 Fig. **Identification of a miR-616-5p and miR-616-3p -binding sites in the c-Myc.**
630 RNAhybrid analysis of c-MYC reference sequence and miR-616. The secondary structure of
631 miRNA-mRNA duplex is shown with miRNA in green and mRNA in red. mfe: minimum free
632 energy.

633

634 S2 Fig. **Association between miR-616 expression and overall survival in human cancer**.
635 Web-based algorithm KM plotter (http://kmplot.com/analysis/) was used to evaluate the
636 association between miR-616 with overall (OS) survival.

637

638 S3 Fig. **Prediction of the effect of miR-616-5p and miR-616-3p on cell viability through their**
639 **6mer seed sequence.** The activity of 6-mer seed of was evaluated in three human (HeyA8-
640 ovarian, H460-lung and H4-brain) and three mouse (M565-liver, 3LL-lung and GL261-brain)
641 cell lines. MiRNAs with low viability (high toxicity) are shown in red and with high viability
642 (low toxicity) are shown in green. Predominantly expressed mature miRNAs (guide miRNA)
643 are shown in dark purple while lesser expressed (passenger miRNA) are shown in light
644 purple. The miRNAs sharing seed sequence with miR-616-5p are also shown.

A

B

CHOP (NM_001195053.1)

miRNA	Other name	Accession number	Sequence 5' to 3'
hsa-miR-616-5p	hsa-miR-616*	MIMAT0003284	ACUCAAAACCCUUCAGUGACUU
hsa-miR-616-3p	hsa-miR-616	MIMAT0004805	AGUCAUUGGAGGGUUUGAGCAG

C

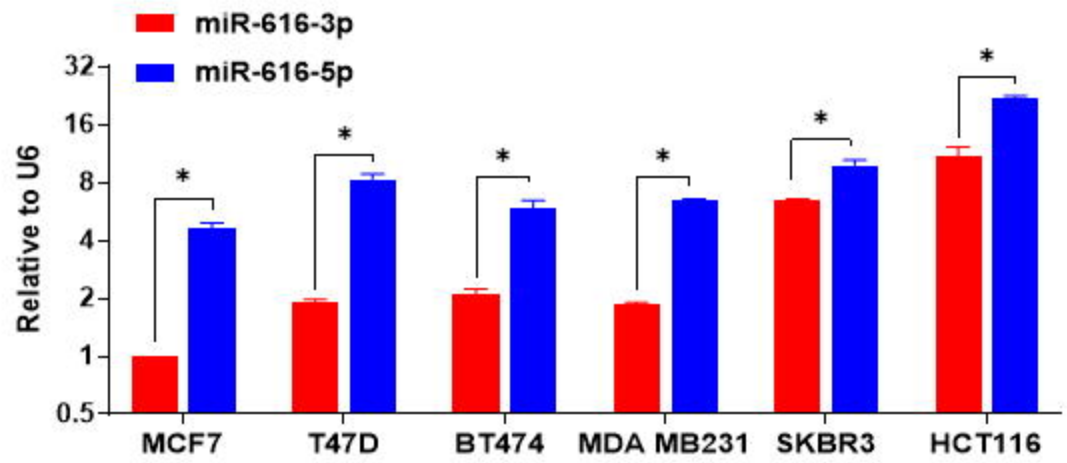

Figure 1

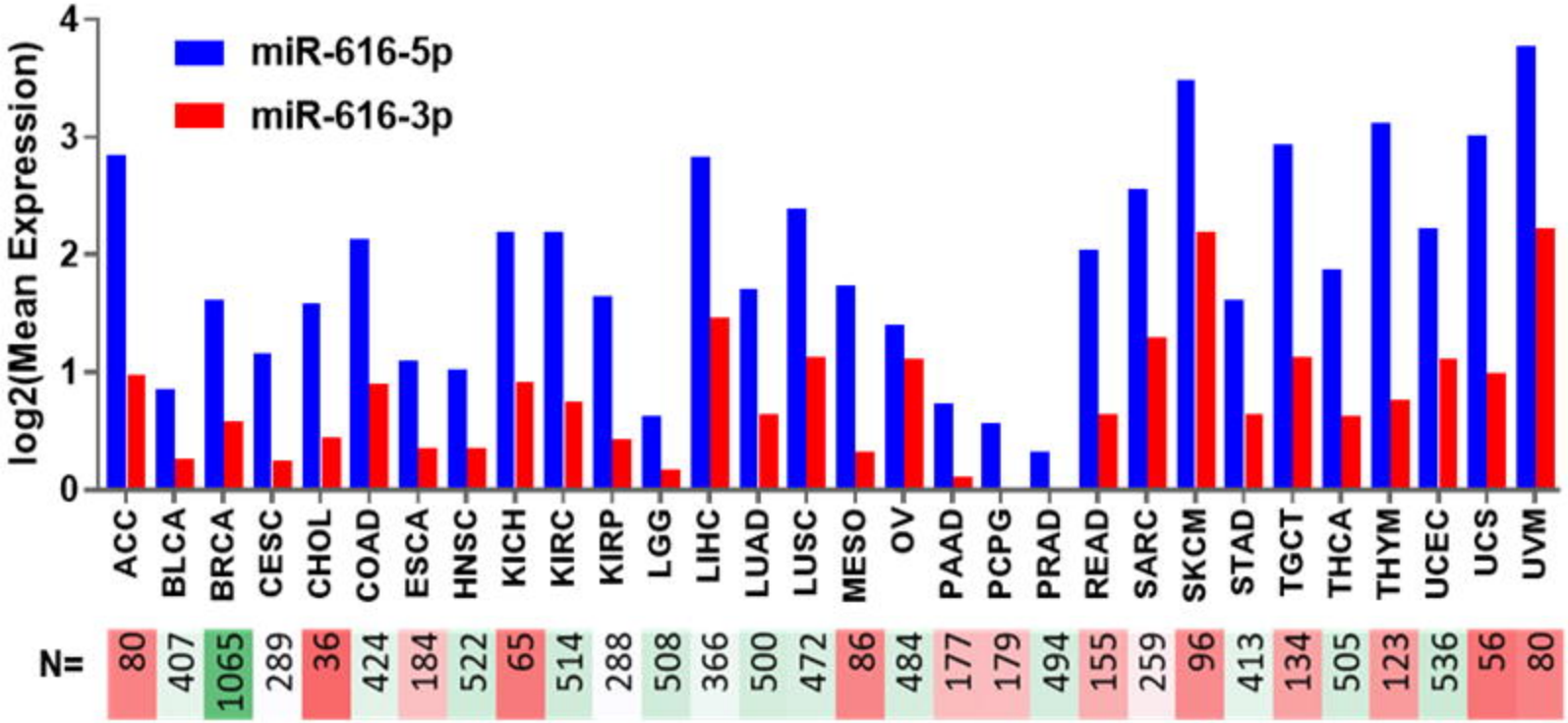
log2(Mean Expression)
miR-616-5p
miR-616-3p
0
1
2
3
4
ACC
BLCA
BRCA
CESC
CHOL
COAD
ESCA
HNSC
KICH
KIRC
KIRP
LGG
LIHC
LUAD
LUSC
MESO
OV
PAAD
PCPG
PRAD
READ
SARC
SKCM
STAD
TGCT
THCA
THYM
UCEC
UCS
UVM
N=
80
407
1065
289
36
424
184
522
65
514
288
508
366
500
472
86
484
177
179
494
155
259
96
413
134
505
123
536
56
80

Figure 2

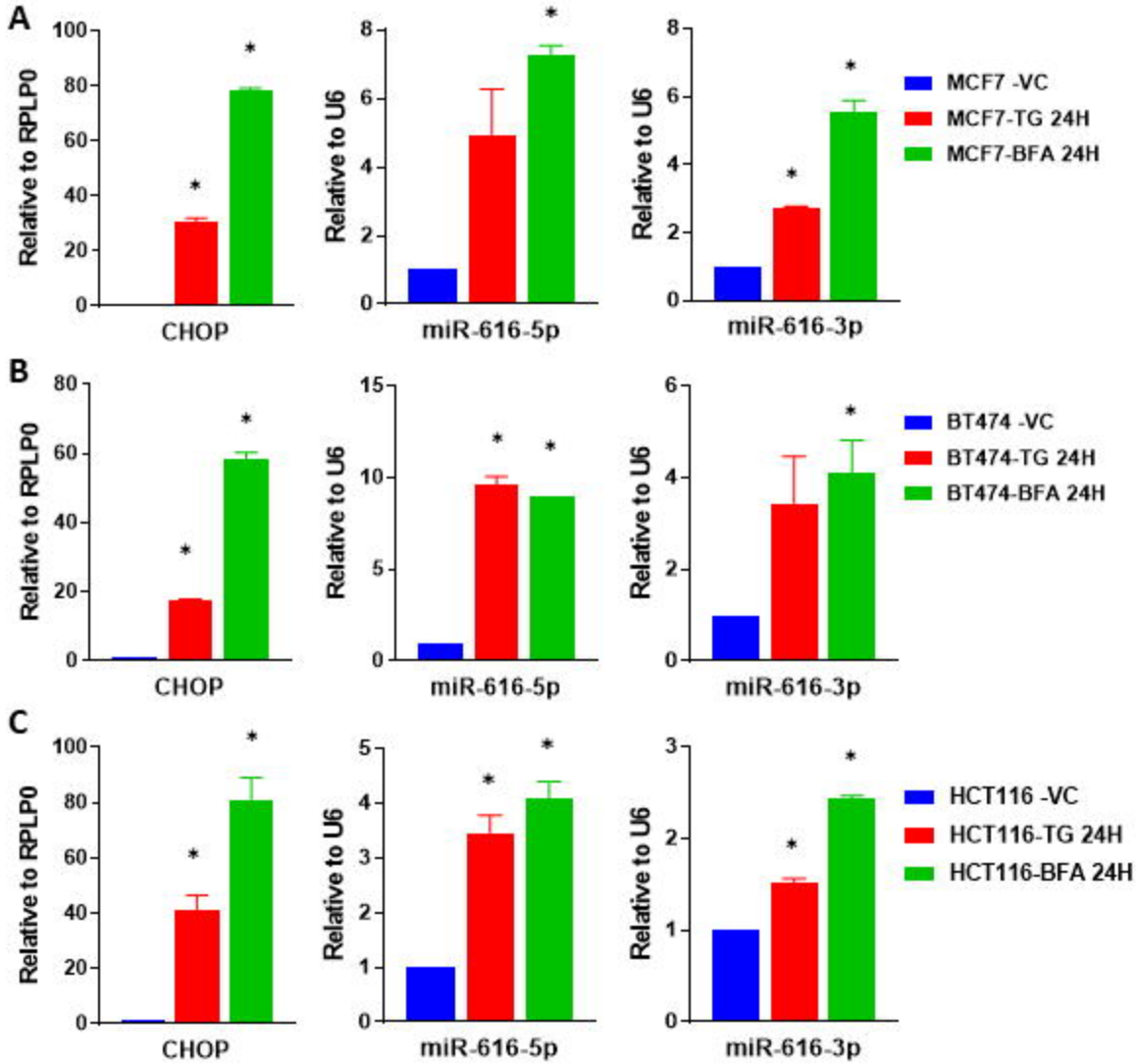
A
Relative to RPLP0
CHOP
Relative to U6
miR-616-5p
miR-616-3p
MCF7 -VC
MCF7-TG 24H
MCF7-BFA 24H
B
BT474 -VC
BT474-TG 24H
BT474-BFA 24H
C
HCT116 -VC
HCT116-TG 24H
HCT116-BFA 24H

Figure 3

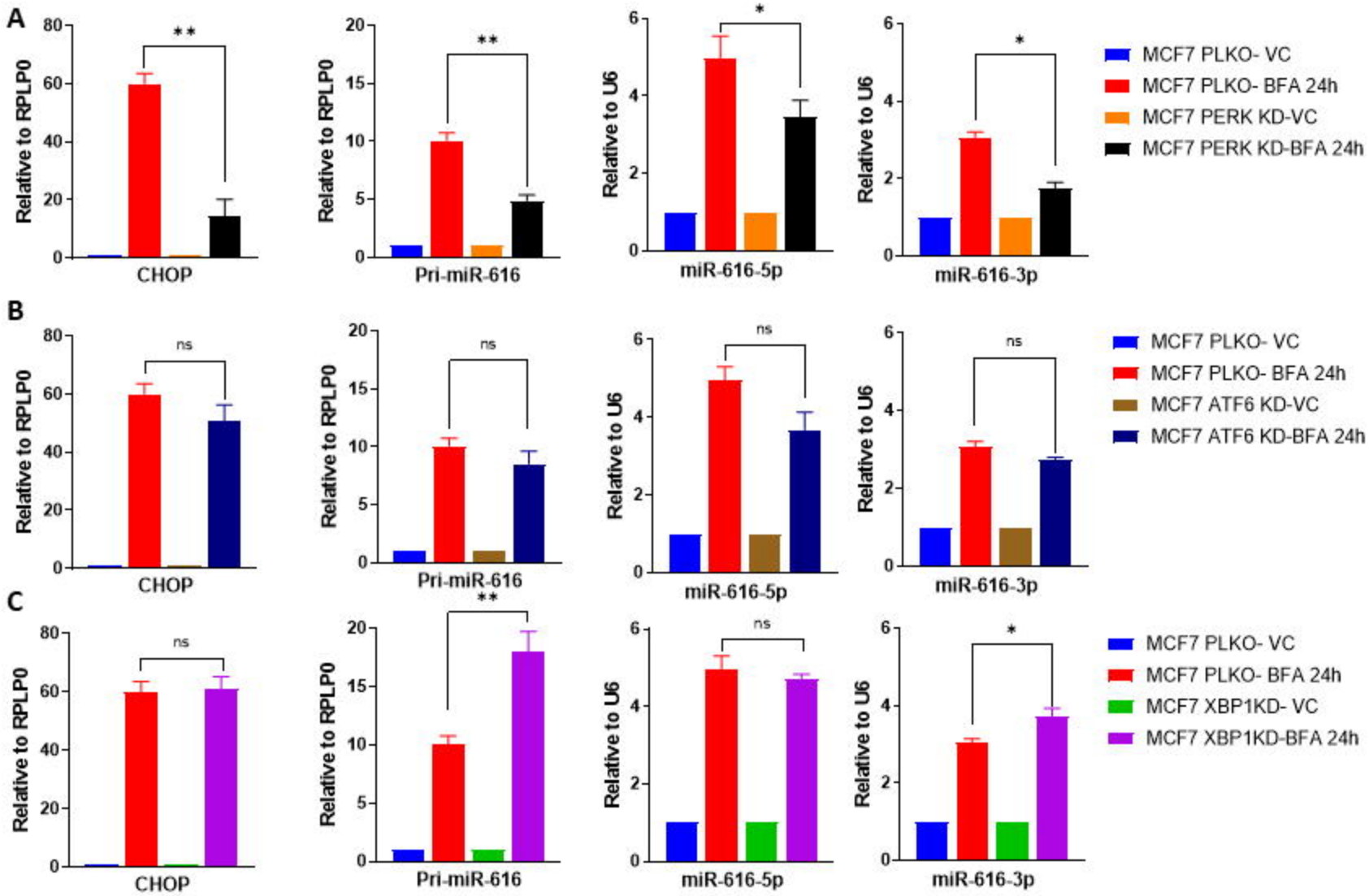
A
B
C
Relative to RPLP0
Relative to U6
CHOP
Pri-miR-616
miR-616-5p
miR-616-3p
**
*
ns
MCF7 PLKO- VC
MCF7 PLKO- BFA 24h
MCF7 PERK KD-VC
MCF7 PERK KD-BFA 24h
MCF7 ATF6 KD-VC
MCF7 ATF6 KD-BFA 24h
MCF7 XBP1KD- VC
MCF7 XBP1KD-BFA 24h

Figure 4

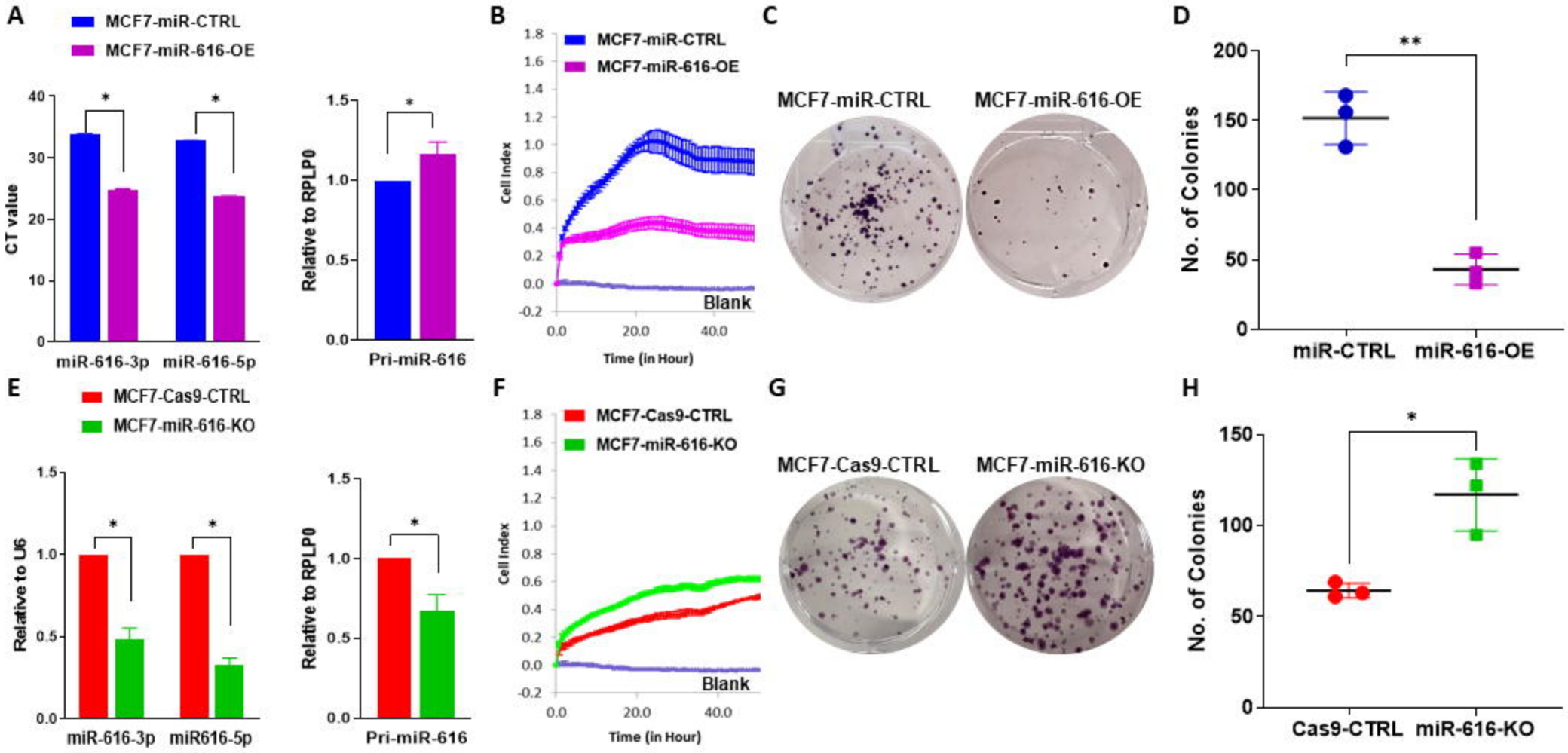
A
MCF7-miR-CTRL
MCF7-miR-616-OE
CT value
miR-616-3p
miR-616-5p
Relative to RPLP0
Pri-miR-616
B
MCF7-miR-CTRL
MCF7-miR-616-OE
Cell Index
Blank
Time (in Hour)
C
MCF7-miR-CTRL
MCF7-miR-616-OE
D
No. of Colonies
miR-CTRL
miR-616-OE
E
MCF7-Cas9-CTRL
MCF7-miR-616-KO
Relative to U6
miR-616-3p
miR616-5p
Relative to RPLP0
Pri-miR-616
F
MCF7-Cas9-CTRL
MCF7-miR-616-KO
Cell Index
Blank
Time (in Hour)
G
MCF7-Cas9-CTRL
MCF7-miR-616-KO
H
No. of Colonies
Cas9-CTRL
miR-616-KO

Figure 5

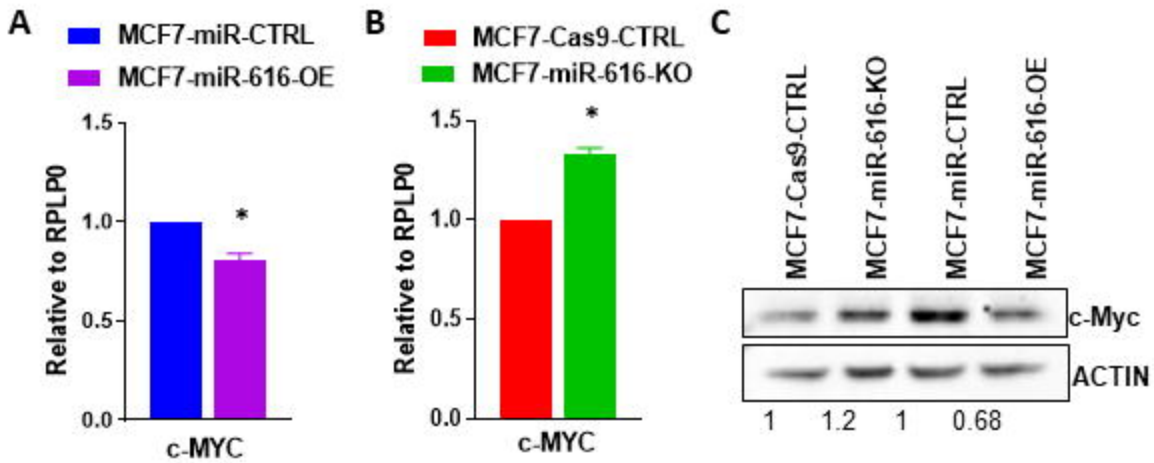
A
MCF7-miR-CTRL
MCF7-miR-616-OE
Relative to RPLP0
1.5
1.0
0.5
0.0
*
c-MYC
B
MCF7-Cas9-CTRL
MCF7-miR-616-KO
Relative to RPLP0
1.5
1.0
0.5
0.0
*
c-MYC
C
MCF7-Cas9-CTRL
MCF7-miR-616-KO
MCF7-miR-CTRL
MCF7-miR-616-OE
c-Myc
ACTIN
1
1.2
1
0.68

Figure 6

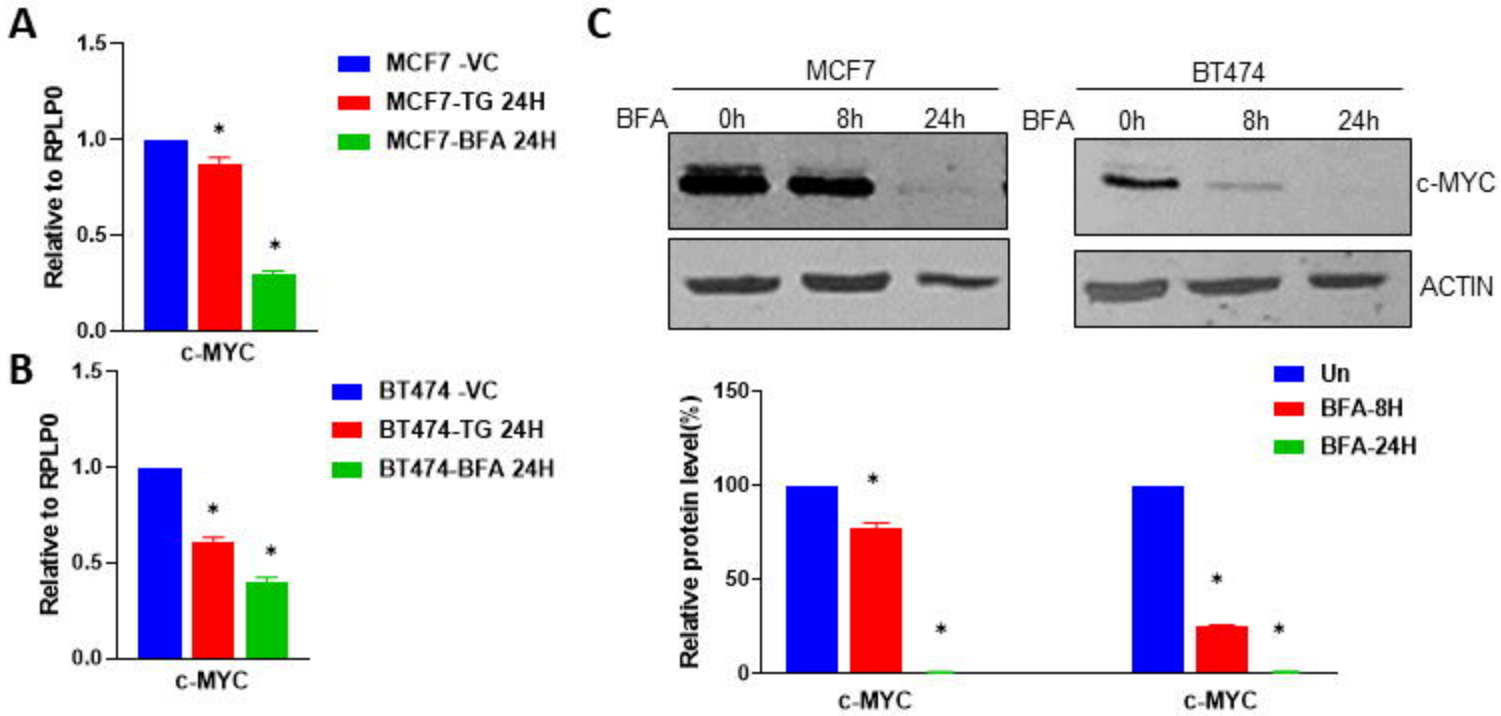
A
1.5
1.0
0.5
0.0
Relative to RPLP0
c-MYC
MCF7 -VC
MCF7-TG 24H
MCF7-BFA 24H
B
1.5
1.0
0.5
0.0
Relative to RPLP0
c-MYC
BT474 -VC
BT474-TG 24H
BT474-BFA 24H
C
MCF7
BT474
BFA
0h
8h
24h
BFA
0h
8h
24h
c-MYC
ACTIN
150
100
50
0
Relative protein level(%)
c-MYC
c-MYC
Un
BFA-8H
BFA-24H

Figure 7

A

miRNA	hsa-miR-616-3p
RefseqID	NM_002467
GeneSymbol	MYC
Binding Site	1525.1546
Score	0.846
Seed	0
Au	0.515
Energy	-20.3
Binding Len	21
Me	-7.719
Phylopstem	0.0
Phylopflank	0.0
Longest Consecutive Pairings	6
Position Of Longest Consecutive Pairings	1
Pairings In 3prime End	4
Position	CDS

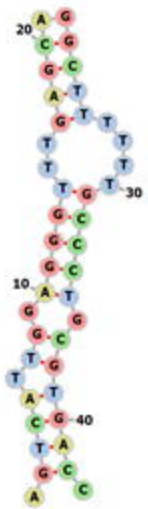

B

```
Target: NM_002467.6
length: 3721
MiRNA: hsa-miR-616-3p
length: 22

mfe: -25.0 kcal/mol
p-value: 1.000000e+00

Position: 1525
target 5'  A    UUUU     G       C 3'
            GCUU    GCCCU C GUGAC
            CGAG    UGGGA G UACUG
miRNA  3' GA    UU       G U     A 5'   mfe: -25.0 kcal/mol
```

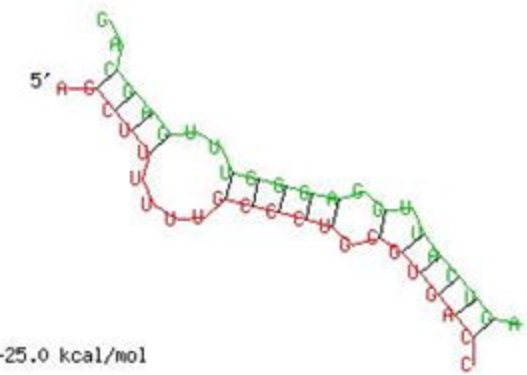

C

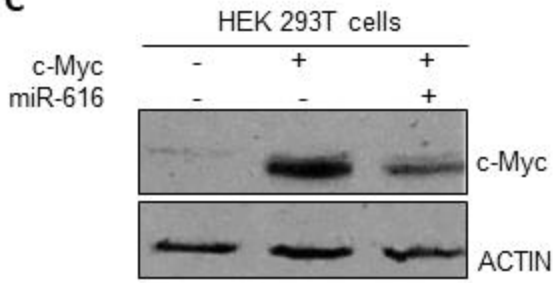

D

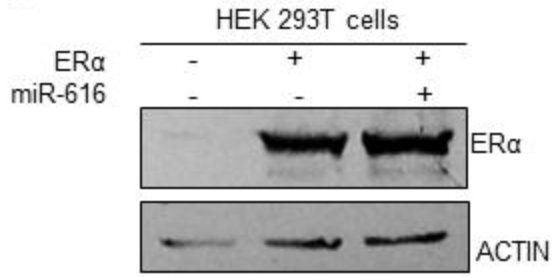

E

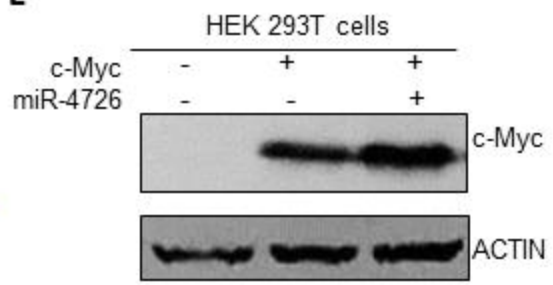

Figure 8

A

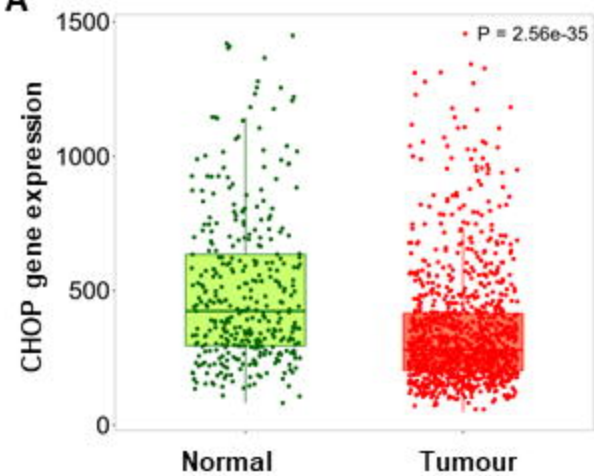

B

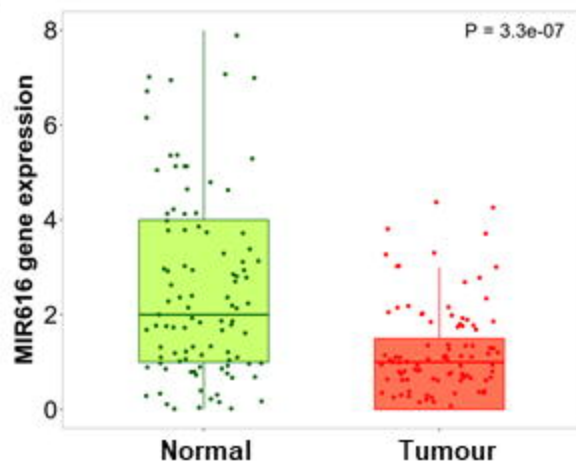

C

Subtypes of breast cancer	Overall survival	
	Hazard Ratio	Logrank P
Luminal A	1.57 (1.08 - 2.27)	**0.01600**
Luminal B	0.81 (0.60 - 1.11)	0.19000
HER2	0.31 (0.16 - 0.61)	**0.00034**
TNBC	0.75 (0.46 - 1.21)	0.24000

Figure 9